AAS 14-238

NEAR OPTIMAL FEEDBACK GUIDANCE DESIGN AND THE PLANAR RESTRICTED THREE-BODY PROBLEM

Joseph Dinius [*], Roberto Furfaro [†‡], Francesco Topputo [§], and Scott Selnick [¶]

In this paper, we present the application of the ZEM/ZEV guidance algorithm to the planar restricted three-body problem (PR3BP). The ZEM/ZEV guidance law as a feedback guidance strategy is presented and applied to the PR3BP. The fuel optimal solution to the PR3BP for a transfer from GTO to L_1 in the Earth-Moon system is presented as a point for comparison, showing the near optimality of the closed-loop guidance approach. Challenges of the approach and strategies for implementation in spacecraft mission design are discussed.

INTRODUCTION

The planar restricted three body problem (PR3BP) has been studied extensively as a model for spacecraft dynamics in the presence of large celestial bodies. Of particular interest to engineers and scientists is how to construct optimal trajectories for accomplishing mission objectives (e.g. minimize fuel consumption, time-to-intercept, or acceleration demand).[1] The current approach for constructing such optimal trajectories is to use nonlinear programming techniques applied to the optimal control problem.[2,3] This approach is open-loop and therefore requires a high-degree of accuracy in modeling the dynamics of the system. Any uncertainty in the underlying models can result in far-from-optimal solutions due to the nonlinear nature of the dynamical systems governing spacecraft flight. To make solutions more robust to modeling uncertainty or perturbation, some form of feedback guidance is desirable.

In this paper, we present a strategy for feedback guidance of spacecraft in the presence of non-constant and nonlinear gravity. We present the (nearly) optimal ZEM/ZEV guidance law.[4] We next present the PR3BP as a simplified model for the gravitational interaction between a spacecraft and two celestial bodies; in this case, the Earth and the Moon. A brief discussion of nonlinear programming (NLP) and collocation techniques for constructing optimal trajectories is discussed to both provide a point of reference to what is currently done in practice and to highlight the need for other techniques in mission trajectory design. The fuel optimal control solution for a spacecraft transferring from a geostationary orbit to an L_1 Lyapunov orbit is computed using methods outlined.

[*] Program in Applied Mathematics, University of Arizona, 617 N Santa Rita Ave, PO Box 210889, Tucson, AZ 85721.
[†] Assistant Professor, Department of Systems and Industrial Engineering, University of Arizona, 1127 E James E. Rogers Way, Room 111, PO Box 210020, Tucson, AZ 85721.
[‡] Assistant Professor, Department of Aerospace and Mechanical Engineering, University of Arizona, 1130 N Mountain Ave, PO Box 210119, Tucson, AZ 85721.
[§] Assistant Professor, Department of Aerospace Science and Technology, Politecnico di Milano, Via La Masa 34, 20156, Milan, Italy.
[¶] Graduate Student, Department of Systems and Industrial Engineering, University of Arizona, 1127 E James E. Rogers Way, Room 111, PO Box 210020, Tucson, AZ 85721.

Finally, we apply the ZEM/ZEV guidance algorithm to the PR3BP and compare the results to the fuel optimal solution. We discuss the challenges of the approach, along with potential strategies for addressing these challenges.

ZEM/ZEV GUIDANCE LAW

In this section, we present the ZEM/ZEV guidance law as an optimal control for the following system of differential equations

$$\begin{aligned} \dot{\mathbf{r}}(t) &= \mathbf{v}(t) \\ \dot{\mathbf{v}}(t) &= \mathbf{g}(t) + \mathbf{u}(t). \end{aligned} \tag{1}$$

For spacecraft applications, the form of the acceleration input, $\mathbf{u}(t)$ has the form of a thrust force, $\mathbf{T}$, divided by vehicle mass, m. This applied force affects the vehicle mass via

$$\dot{m}(t) = -\frac{m(t)||\mathbf{u}(t)||}{I_{sp}g_0}, \tag{2}$$

where $||\cdot||$ denotes the Euclidean norm, I_{sp} the motor specific impulse and g_0 the gravitational constant. For most applications, there is assumed to be a maximum available thrust, T_{max}, such that for all time t

$$0 \leq ||\mathbf{u}(t)|| \leq \frac{T_{max}}{m(t)}. \tag{3}$$

The ZEM/ZEV guidance law $\mathbf{u}^*(t)$, equivalently known as Constrained Terminal Velocity Guidance (CTVG),[4] is developed as the optimal control for Eqs. (1) with cost

$$J = \frac{1}{2}\int_{t_0}^{t_f} ||\mathbf{u}(\tau)||^2 \mathrm{d}\tau, \tag{4}$$

and terminal (boundary) conditions (5)

$$\begin{aligned} \mathbf{r}(t_0) = \mathbf{r}_0, \mathbf{r}(t_f) = \mathbf{r}_f \\ \mathbf{v}(t_0) = \mathbf{v}_0, \mathbf{v}(t_f) = \mathbf{v}_f. \end{aligned} \tag{5}$$

As can be seen from the structure of the cost function of Eq. (4), the ZEM/ZEV guidance law minimizes the acceleration effort required for meeting mission objectives (i.e. arriving at a specific point with specific velocity). A nice development of the full derivation has been previously provided,[4,5] therefore we present only the solution. If we define $t_{go} = t_f - t$ as the time before reaching the terminal time from the present one, then the ZEM/ZEV guidance law is

$$\begin{aligned} \mathbf{u}^*(t) &= \frac{6}{t_{go}^2}\mathbf{r}_{ZEM} - \frac{2}{t_{go}}\mathbf{v}_{ZEV} \\ \mathbf{r}_{ZEM} &= \mathbf{r}_f - \left(\mathbf{r}(t) + \mathbf{v}(t)t_{go} + \int_t^{t_f}(\tau - t)\mathbf{g}(\tau)d\tau\right) \\ \mathbf{v}_{ZEV} &= \mathbf{v}_f - \left(\mathbf{v}(t) + \int_t^{t_f}\mathbf{g}(\tau)d\tau\right). \end{aligned} \tag{6}$$

Applying the acceleration saturation condition of Eq. (3), we arrive at the *limited* ZEM/ZEV guidance law

$$\mathbf{u}^*_{ZEM/ZEV}(t) = \mathrm{sat}_{T_{max}/m}\left\{\frac{6}{t_{go}^2}\mathbf{r}_{ZEM} - \frac{2}{t_{go}}\mathbf{v}_{ZEV}\right\}. \tag{7}$$

A brief discussion of Eqs. (6) and (7) is useful here. The control derived above computes optimal gains to apply to the zero-effort-miss ($\mathbf{r}_{ZEM}$) and zero-effort velocity ($\mathbf{v}_{ZEV}$), which are, respectively, the n-dimensional vector difference between our desired terminal miss (velocity) at the point of closest approach. For the problem to be discussed subsequently, the number of spatial dimensions is $n = 2$. The point of closest approach occurs at time t_{go}.

Computing Time-to-Go, t_{go}

The time-to-go, t_{go}, is computed using the Hamiltonian, $H(t)$, for the optimal control problem defined in Eqs. (1), (4) and (5). Given the optimal control from Eq. (6), the Hamiltonian is

$$H(t) = \frac{1}{2}||\mathbf{u}^*(t)||^2 + \mathbf{u}^{*T}(t)\mathbf{g}(t) + \mathbf{p}_{\mathbf{r}}^T(t_f)\mathbf{v}(t), \tag{8}$$

where $\mathbf{p}(t) \equiv (\mathbf{p}_{\mathbf{r}}^T(t)\ \mathbf{p}_{\mathbf{v}}^T(t))^T$ is the solution to the *costate equations*[5] in the construction of the optimal control of Eq. (6),

$$\dot{\mathbf{p}}(t) = -\frac{\partial H}{\partial \mathbf{x}},$$
$$\mathbf{x}(t) \equiv \begin{pmatrix} \mathbf{r}(t) \\ \mathbf{v}(t) \end{pmatrix}.$$

Along the optimal trajectory, $H(t_f) = 0$.[5] Therefore, t_{go} is computed as the difference between the final time, t_f, computed by $H(t_f) = 0$ and the current time, t. Closed-form solutions for t_{go} exist under the assumptions of constant[6] and negligible[4] gravities. However, in the more general setting, as in our problem of interest, such closed form solutions are of small utility. In general, numerical methods must be used to find roots of the nonlinear equation in Eq. (8). A root-finding algorithm (e.g. conjugate-gradient or Newton-Raphson) can be used to find the zero, t_f, of Eq. (8). Equivalently, a global minimizer can be used to find the time at which the (Euclidean) norm of $\mathbf{\Delta}$ is minimized, where

$$\mathbf{\Delta} \equiv \begin{pmatrix} \mathbf{r}_f - \mathbf{r}_{ZEM} \\ \mathbf{v}_f - \mathbf{v}_{ZEV} \end{pmatrix}.$$

The latter approach is simpler to implement numerically and more robust, therefore it is used for subsequent numerical analyses.

PLANAR RESTRICTED THREE BODY PROBLEM (PR3BP)

The PR3BP describes the motion of a body (of insignificant mass) in the presence of two primary bodies. The coordinate frame chosen for convenience, and to exploit inherent symmetry, is the non-inertial rotating frame in which the two primary bodies' locations are fixed along the x-axis. This coordinate frame is known as the *synodic frame*. The location of the more massive body, P_1, is taken to be the origin, while the second body's, P_2's, position is $(1, 0)$. The dimensionless

equations-of-motion for the PR3BP expressed in the synodic frame are then

$$\begin{aligned}
\dot{x}(t) &= v_x(t) \\
\dot{v}_x(t) &= 2v_y(t) + \frac{\partial \Omega}{\partial x} \\
\dot{y}(t) &= v_y(t) \\
\dot{v}_y(t) &= -2v_x(t) + \frac{\partial \Omega}{\partial y} \\
\Omega &= \frac{1}{2}(x^2 + y^2) + \frac{1-\mu}{r_1} + \frac{\mu}{r_2} + \frac{1}{2}\mu(1-\mu).
\end{aligned} \tag{9}$$

In Eq. (9), r_1 is the distance of the third body from P_1, r_2 the distance of the third body from P_2 and μ is the dimensionless mass parameter (where m_1, m_2 are the masses of P_1, P_2, respectively)

$$\begin{aligned}
\mathbf{r}_{P_1} &= \begin{pmatrix} 0 & 0 \end{pmatrix}^T \\
\mathbf{r}_{P_2} &= \begin{pmatrix} 1 & 0 \end{pmatrix}^T \\
\mathbf{r} &= \begin{pmatrix} x & y \end{pmatrix}^T \\
r_1 &= ||\mathbf{r} - \mathbf{r}_{P_1}|| \\
r_2 &= ||\mathbf{r} - \mathbf{r}_{P_2}|| \\
\mu &= \frac{m_2}{m_1 + m_2}.
\end{aligned}$$

The dynamics of the PR3BP have many interesting structures to exploit in the optimization of trajectories; particularly, the notions of *stable* and *unstable manifolds* and the heteroclinic connections between them (see Guckenheimer and Holmes[7]). It is important to note here that gravity of the form in Eq. (1) is a nonlinear function of position* in Eq. (9). Therefore, the ZEM/ZEV guidance law of Eq. (7) will not be optimal, strictly speaking, given the construction of the previous section. This will be discussed later.

FUEL OPTIMAL GTO TO L_1 TRANSFER IN THE EARTH-MOON SYSTEM

The fuel optimal control $\{\mathbf{u}^*_{FO}(t)\}$ is the time-history of the control law which minimizes the performance index

$$J = \int_{t_0}^{t_f} \|\mathbf{u}(t)\| \mathrm{d}t$$

from an initial time t_0 to final time t_f for the PR3BP of Eq. (9). The computation of the time-history $\{\mathbf{u}^*_{FO}(t)\}$ is done using nonlinear programming (NLP) methods for open-loop optimization. A brief discussion of the implementation of these methods for computing $\{\mathbf{u}^*_{FO}(t)\}$ is presented in the next section.

NLP and Collocation: Arbitrary Order Gauss–Lobatto Method

The NLP method chosen for computations is the Gauss-Lobatto method. Herman and Conway[8] demonstrated that higher order Gauss-Lobatto methods are more robust and more efficient than lower-order Hermite-Simpson schemes, but in the framework proposed in Tang and Conway,[9]

*The construction of the optimal control assumed that gravity is a function of time only; see Eq. (1).

a detailed derivation of the formulas was required when extending to arbitrarily high order. In Williams,[10] an alternative framework for unifying arbitrary higher-order methods was presented. In this approach, continuity time $[t_0, t_f]$ is discretized to a large number of subintervals, whose endpoints are determined by *nodes* $\{\tau_0, \tau_1, \cdots, \tau_n\}$. Within each subinterval the state variables are approximated by a local Hermite interpolation polynomial. The Legendre-Gauss-Lobatto (LGL) discrete points ξ_j are used to improve both interpolating precision and quadrature performance. Fig. 1 illustrates the location of 3, 5 and 7 LGL points, respectively.

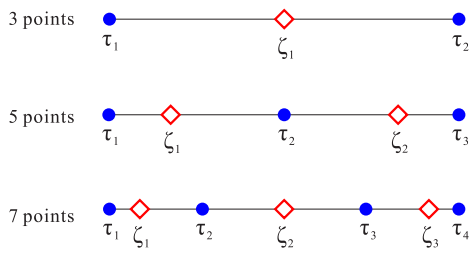

Figure 1. 3, 5 and 7 Legendre-Gauss-Lobatto points.

With reference to Fig. 1, the blue points are the nodes, which are defined by

$$\tau_j = \xi_{2j-1}, j = 1, \ldots, (n+1)/2,$$

while the red diamond are the *collocation points*, denoted as

$$\zeta_j = \xi_{2j}, j = 1, \ldots, (n-1)/2,$$

so there is one collocation point between every two adjacent nodes. The nodes are used for constructing interpolation polynomials while the collocation points are used for formulating the defect constraints for the NLP optimization problem. When there are 3 points, the Gauss-Lobatto method degenerates to the Hermite-Simpson method.

The state in the ith subinterval is approximated by the nth degree Hermite interpolating polynomial:

$$x(\tau) \approx a_0 + a_1\tau + a_2\tau^2 + a_3\tau^3 + \cdots + a_n\tau^n, \tau \in [-1, 1]$$

where the coefficients of Hermite interpolating polynomial $a = [a_0, a_1, a_2, \ldots, a_n]^T$ are determined by using the values of the states and vector field at the points τ_j; i.e.

$$\begin{pmatrix} 1 & \tau_1^1 & \tau_1^2 & \cdots & \tau_1^{n-1} & \tau_1^n \\ 1 & \tau_2^1 & \tau_2^2 & \cdots & \tau_2^{n-1} & \tau_2^n \\ \vdots & \vdots & \vdots & \vdots & \vdots & \vdots \\ 1 & \tau_{\frac{n+1}{2}}^1 & \tau_{\frac{n+1}{2}}^2 & \cdots & \tau_{\frac{n+1}{2}}^{n-1} & \tau_{\frac{n+1}{2}}^n \\ 0 & 1 & 2\tau_1^1 & \cdots & (n-1)\tau_1^{n-2} & n\tau_1^{n-1} \\ \vdots & \vdots & \vdots & \vdots & \vdots & \vdots \\ 0 & 1 & 2\tau_{\frac{n+1}{2}}^1 & \cdots & (n-1)\tau_{\frac{n+1}{2}}^{n-2} & n\tau_{\frac{n+1}{2}}^{n-1} \end{pmatrix} \begin{pmatrix} a_0 \\ a_1 \\ a_2 \\ \vdots \\ \vdots \\ a_{n-1} \\ a_n \end{pmatrix} = \begin{pmatrix} x(\tau_1) \\ x(\tau_2) \\ \vdots \\ x(\tau_{\frac{n+1}{2}}) \\ \frac{h}{2}f(\tau_1) \\ \vdots \\ \frac{h}{2}f(\tau_{\frac{n+1}{2}}) \end{pmatrix} \tag{10}$$

In Eq. (10), it is assumed that the dynamics are of the form

$$\dot{x}(t) = f(x(t), u(t), t).$$

Let Eq. (10) be written as $Aa = b$. The term A depends only on the number and location of node points, whereas b is a concatenated vector of state and vector field values. Thus, given a vector of states, the coefficients of the Hermite interpolation in the ith subinterval, a, can be found by $a = [A]^{-1}b$. The values of the states located at collocation points are then

$$x(\zeta_j) = \begin{pmatrix} 1 & \zeta_1 & \zeta_1^2 & \dots & \zeta_1^n \\ 1 & \zeta_2 & \zeta_2^2 & \dots & \zeta_2^n \\ \vdots & \vdots & \vdots & \dots & \vdots \\ 1 & \zeta_{\frac{n-1}{2}} & \zeta_{\frac{n-1}{2}}^2 & \dots & \zeta_{\frac{n-1}{2}}^n \end{pmatrix} [A]^{-1}b = \Phi b, \tag{11}$$

for $j = 1, 2, \dots, (n-1)/2$. The derivative of the Hermite interpolating polynomial located at the collocation points are given by

$$\dot{x}(\zeta_j) = \begin{pmatrix} 0 & 1 & 2\zeta_1 & \dots & n\zeta_1^{n-1} \\ 0 & 1 & 2\zeta_2 & \dots & n\zeta_2^{n-1} \\ \vdots & \vdots & \vdots & \dots & \vdots \\ 0 & 1 & 2\zeta_{\frac{n-1}{2}} & \dots & n\zeta_{\frac{n-1}{2}}^{n-1} \end{pmatrix} [A]^{-1}b = \Phi' b, \tag{12}$$

for $j = 1, 2, \dots, (n-1)/2$.

In this form the matrix of Φ and Φ' are constants, thus a system of $(n-1)/2$ constraints per interval are obtained

$$\begin{aligned} \Delta_i &= \dot{x}(\zeta_j) - \frac{h}{2} f(x(\zeta_j), u(\zeta_j), t(\zeta_j)) \\ &= \Phi' b - \frac{h}{2} f(\Phi b, u(\zeta_j), t(\zeta_j)) \end{aligned} \tag{13}$$

and the analytic Jacobian for the defect constraints can be derived by the chain rule as

$$\begin{aligned} &\frac{\partial \Delta_i}{\partial [x(\tau_j), u(\tau_j)]_i} = \Phi' \frac{\partial b}{\partial [x(\tau_j), u(\tau_j)]_i} \\ &- \frac{h}{2} \left[\frac{\partial f}{\partial x(\zeta_j)} \Phi \frac{\partial b(\zeta_j)}{\partial [x(\tau_j), u(\tau_j)]_i} + \frac{\partial f}{\partial u(\zeta_j)} \frac{\partial u(\zeta_j)}{\partial [x(\tau_j), u(\tau_j)]_i} \right] \end{aligned} \tag{14}$$

If the final transfer time t_f is variable (i.e. the terminal time is unconstrained), within each segment, the analytic Jacobian of t_f can be written as

$$\begin{aligned} \frac{\partial \Delta_i}{\partial t_f} &= \Phi' \frac{\partial b}{\partial h} \frac{\partial h}{\partial t_f} \\ &- \left[\frac{1}{2} \frac{\partial h}{\partial t_f} f(x(\zeta_j), u(\zeta_j)) + \frac{h}{2} \frac{\partial f}{\partial x(\zeta_j)} \Phi \frac{b}{h} \frac{h}{t_f} \right] \end{aligned} \tag{15}$$

A graphical illustration of the Jacobian structure with free final time t_f is given in Fig. 2.

In Fig. 2, each segment has the same Jacobian module, thus Eqs. (14) and (15) can be calculated off-line and stored in a file before solving the NLP. In this way, the computational time can be reduced by about 50% compared to the use of finite difference approximation.

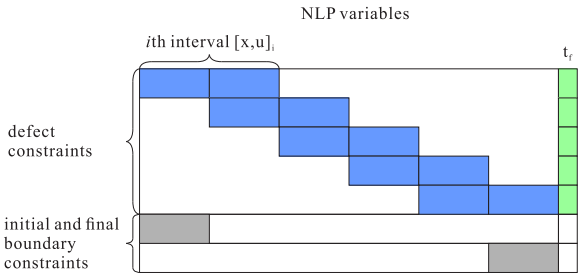

Figure 2. Jacobian structure for 3 order Gauss-Lobatto method.

Table 1. Scaling parameters for the PR3BP: Earth-Moon System

Parameter	Scaling	Label
Mass	0.01215 (dim)	μ
Time	3.757e5 (sec)	TU
Length	3.850e5 (km)	LU

Simulation Details

For convenience, the PR3BP is solved in dimensionless coordinates. Table 1 shows the scaling parameters.

Figure 3 shows the trajectory with fuel optimal control $\{u^*_{FO}(t)\}$ for a geostationary transfer orbit to L_1 Lyapunov transfer computed using the methods of the previous section. The initial mass of the spacecraft is $m_0 = 1000$ kg, the motor specific impulse I_{sp} is 3000 sec and the maximum motor thrust is $T_{max} = 0.5$ N.[11] The "bang-bang" control structure observed is as expected. This trajectory provides a point for comparison with closed-loop guidance using the control $\mathbf{u}^*_{ZEM/ZEV}(t)$ of Eq. (7).

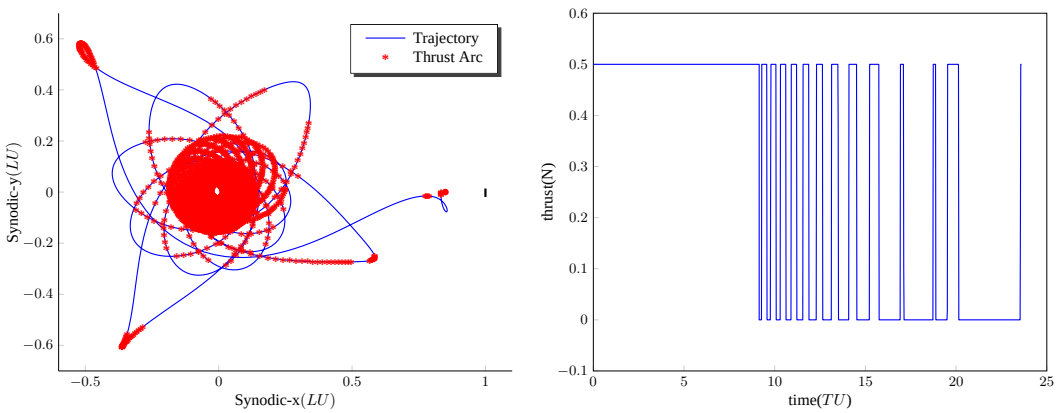

Figure 3. Left: Fuel optimal trajectory for transfer from GTO to L_1 halo orbit. Right: Time history of control thrust for optimal trajectory.

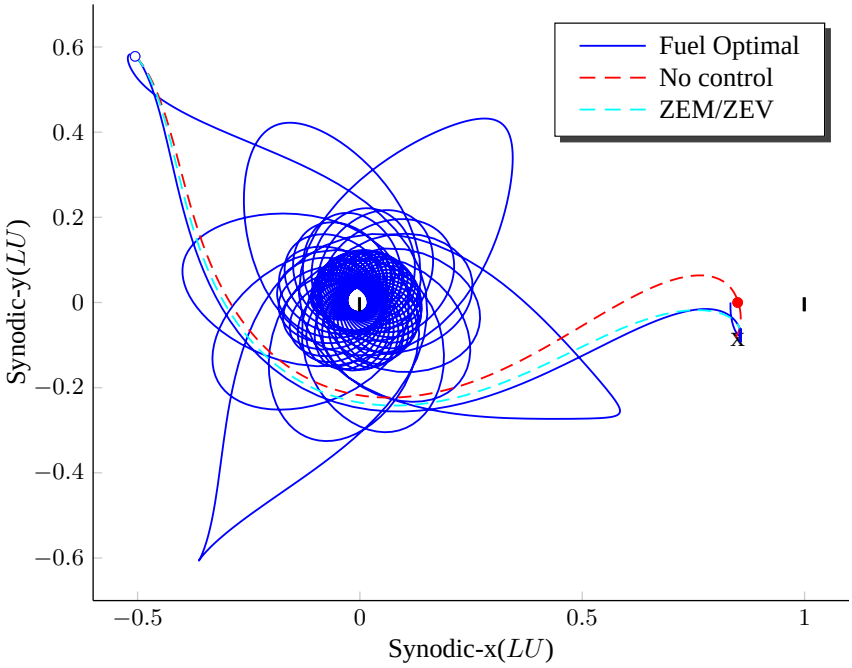

Figure 4. Trajectory comparison of fuel optimal trajectory with ZEM/ZEV guidance and uncontrolled trajectories. The starting point (o) is selected near a phase point where thrust is needed for course correction in the fuel optimal trajectory. The endpoint (x) is selected as the next phase point where thrust is needed for course correction in the fuel optimal trajectory.

COMBINING ZEM/ZEV GUIDANCE AND THE PR3BP

The ZEM/ZEV guidance algorithm can be applied using a point along the fuel optimal trajectory as an initial condition. The comparison of the fuel optimal trajectory with both ZEM/ZEV and no control is shown in Figure 4. For the segment of the trajectory considered, the fuel optimal and ZEM/ZEV trajectories match favorably when compared to the uncontrolled trajectory. How to select the starting and ending points for applying the ZEM/ZEV algorithm is important. The algorithm was found to be suboptimal guiding through inflections in the trajectory; that is, where points in the fuel optimal trajectory required thrust for course correction. Figure 5 shows the accelerations commanded for the ZEM/ZEV algorithm as a function of time-to-go, t_{go}, and the comparison of mass consumption. As would be expected, ZEM/ZEV is not fuel efficient. However, ZEM/ZEV reduces time-of-flight (over the segment considered) by $\sim 3\%$. As an entry point to future analyses regarding robustness and application to more complex gravity environments (e.g. ephemeris models), the results thus far look promising. The ZEM/ZEV guidance law provides regular updates for course correction and can be made more robust through modeling fidelity and incorporation of measurements.

The strategy then becomes: how is the ZEM/ZEV guidance algorithm best employed? In future works, we aim to integrate the ZEM/ZEV guidance algorithm with a global optimizer to identify optimal waypoint construction as in Sharma.[12] We also aim to perturb optimal solutions found via open-loop strategies, both with gravitational perturbations and perturbations to initial condition, (see Zhang *et. al*[11]) and supplement the solution with ZEM/ZEV for course correction.

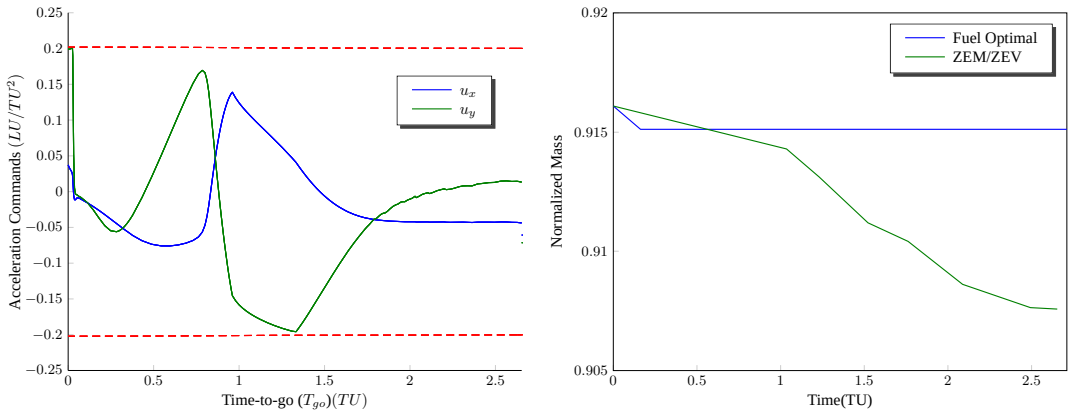

Figure 5. Left: Acceleration time history versus time-to-go. The acceleration limits are plotted in dashed. Right: Comparison of mass consumption for both the fuel optimal and ZEM/ZEV over the trajectory segments considered. As expected, the ZEM/ZEV trajectory is not as mass-efficient.

CONCLUDING REMARKS

In this paper the ZEM/ZEV guidance algorithm has been applied to the case of a low-thrust transfer from the GTO to a Lyapunov orbit about L_1. The dynamics considered are those of the restricted three-body problem with the Earth and Moon as primaries. As expected, the closed-loop guidance method is suboptimal. However, it succeeds in guiding the spacecraft properly to the final target. The ZEM/ZEV algorithm should be thought of as a *component* of the solution for low-thrust transfers, not the complete solution. The algorithm can be used to drive spacecraft back onto fuel optimal trajectories when errors are present (e.g. navigation, sensor, or modeling uncertainties). Future work will be performed to address the optimal selection of waypoints.

REFERENCES

[1] G. Mingotti, F. Topputo, and F. Bernelli-Zazzera, "Optimal Low-Thrust Invariant Manifold Trajectories via Attainable Sets," *Journal of Guidance, Control, and Dynamics*, Vol. 34, November–December 2011, pp. 1644–1656, 10.1007/s10569-011-9343-5.

[2] G. Mingotti, F. Topputo, and F. Bernelli-Zazzera, "Efficient Invariant-Manifold, Low-Thrust Planar Trajectories to the Moon," *Communication in Nonlinear Science and Numerical Simulation*, Vol. 17, No. 2, 2012, pp. 817–831, 10.1016/j.cnsns.2011.06.033.

[3] F. Topputo, "On Optimal Two-Impulse Earth–Moon Transfers in a Four-Bod Model," *Celestial Mechanics and Dynamical Astronomy*, Vol. 117, No. 3, 2013, pp. 279–313, 10.1007/s10569-013-9513-8.

[4] Y. Guo, M. Hawkins, and B. Wie, "Optimal Feedback Guidance Algorithms for Planetary Landing and Asteroid Intercept," *AAS/AIAA Astrodynamics Specialist Conference*, 2011, pp. 2011–588.

[5] D. E. Kirk, *Optimal control theory: an introduction*. DoverPublications. com, 2012.

[6] C. N. DSouza, "An optimal guidance law for planetary landing," *Paper No. AIAA*, 1997, pp. 97–3709.

[7] J. Guckenheimer and P. Holmes, *Nonlinear oscillations, dynamical systems, and bifurcations of vector fields*. Springer-Verlag, 1983.

[8] A. L. Herman and B. A. Conway, "Direct optimization using collocation based on high-order Gauss-Lobatto quadrature rules," *Journal of Guidance, Control, and Dynamics*, Vol. 19, No. 3, 1996, pp. 592–599.

[9] S. Tang and B. A. Conway, "Optimization of low-thrust interplanetary trajectories using collocation and nonlinear programming," *Journal of Guidance, Control, and Dynamics*, Vol. 18, No. 3, 1995, pp. 599–604.

[10] P. Williams, "Hermite-Legendre-Gauss-Lobatto Direct Transcription in Trajectory Optimization," *Journal of guidance, control, and dynamics*, Vol. 32, No. 4, 2009, pp. 1392–1395.

[11] C. Zhang, F. Topputo, F. Bernelli-Zazzera, and Y.-S. Zhao, "An Exploration of Numerical Methods for Low-Thrust Trajectory Optimization in N-Body Models," *64th International Astronautical Congress*, 2013.

[12] R. Sharma, S. R. Vadali, and J. E. Hurtado, "Optimal Nonlinear Feedback Control Design Using a Waypoint Method," *Journal of Guidance, Control, and Dynamics*, Vol. 34, No. 3, 2011, pp. 698–705.